Journal of Molecular Modeling (2018) 24: 267
https://doi.org/10.1007/s00894-018-3807-4

ORIGINAL PAPER

Mechanism and kinetic analysis of PCDD/Fs formation from aliphatic hydrocarbons (C_2H_2, C_2H_4, C_3H_6, C_4H_8) precursors

Zhengyang Gao[1] · Yao Sun[1] · Minghui Li[1] · Wentao Han[1]

Received: 5 June 2018 / Accepted: 21 August 2018 / Published online: 31 August 2018
© Springer-Verlag GmbH Germany, part of Springer Nature 2018

Abstract

Density functional theory calculations were performed to gain insight into the mechanism and kinetic studies of homogeneous gas-phase formation of polychlorinated dibenzodioxins and polychlorinated dibenzofurans (PCDD/Fs) via aliphatic hydrocarbons (C_2H_2, C_2H_4, C_3H_6 and C_4H_8). The calculated results demonstrated that the intra-annular elimination of H is the rate-determining step throughout the reaction chain; the presence of ortho-Cl increases the abstraction barrier of arene H and decreases the reactivity of the molecule. The phenoxy radicals undergoes dimerization via carbon–carbon or carbon–oxygen coupling to form PCDD/Fs and the two coupling pathways are competitive. Our work indicates that aliphatic hydrocarbons are less reactive precursors in PCDD/F formation compared with chlorophenoxy radicals and phenoxy radicals among primary precursors of PCDD/Fs. The results presented here could be used to evaluate the contribution of aliphatic hydrocarbons acting as precursors to PCDD/Fs formation.

Keywords Aliphatic hydrocarbons precursors · Polychlorinated dibenzo-p-dioxins · Reaction mechanism · Rate constants

Introduction

With the accelerating urbanization process, the capacity needed for sewage treatment is also expanding rapidly, and sewage sludge output has increased in recent decades [1]. Sewage sludges are residues originating from the treatment of wastewater released from various sources including industries, businesses, medical facilities, street runoff and homes [2]. The compositions of the sludges are complex; however, they contain metals, pathogens, and organic pollutants, which aggravate soil and accululate through the food chain, ultimately affecting the health and survival of human beings [3]. Due to the tremendous volume of sludge production, several processing solutions have been put forward. The conventional solution is to use landfill, but this wastes a lot of resources, and the toxic substances contained in the sludge have a detrimental effect on the surrounding groundwater sources and ecosystems [4]. Sludge can be also processed by anaerobic bacteria fermentation to produce biogas, and the waste residue can be used as organic fertilizers and soil amendment simultaneously, but this method has the disadvantages of being time consuming, requiring high original investment and being difficult to generalize [5]. Incineration technology is attractive due to its capacity to continuously reduce garbage volume, kill vast numbers of microbial pathogens such as bacteric and viruses contained in garbage, and to recycle heat and metal simultaneously [3]. Incineration technology is a better way to deal with sludge because dry sludge contains abundant organic matter and other combustible components, but incineration produces highly toxic dioxins, which contravenes current regulations [6, 7].

Dioxins have attracted widespread attention in the scientific community due to their characteristics of environmental persistence, bioaccumulation, and far reaching and high toxicity [8, 9]. Researchers have conducted many investigations and studies on the emission of multifarious dioxin waste incineration [10]. Three major mechanisms of polychlorinated dibenzodioxin and polychlorinated dibenzofuran (PCDD/F) formation have been proposed and assessed experimentally by numerous investigators: PCDD/Fs are already present in the sludge and are incompletely destroyed or transformed

Electronic supplementary material The online version of this article (https://doi.org/10.1007/s00894-018-3807-4) contains supplementary material, which is available to authorized users.

✉ Yao Sun
sunnyao07@163.com

[1] School of Energy and Power Engineering, North China Electric Power University, Baoding 071003, China

during combustion [11]; PCDD/Fs are produced from related chlorinated precursors such as chlorinated phenols and chlorinated benzenes [12]; PCDD/Fs are formed via de novo synthesis from carbon, hydrogen, oxygen and chlorine through elementary reactions [13]. The homogeneous gas-phase mechanism of PCDD/F formation is one of the most important mechanisms of dioxin formation in municipal solid waste (MSW) incinerators [14, 15]. To date, the most researched pathways involve formation through de novo synthesis from chlorinated aliphatic hydrocarbons and chlorinated aromatic precursors. However, to the best of our knowledge, few reports provide systemic information on de novo synthesis from aliphatic hydrocarbons. Therefore, studying aliphatic hydrocarbons as precursors of PCDD/F formation could suggest means to suppress the formation of dioxins at source.

In this study, quantum chemistry calculations in the framework of the density functional theory (DFT) were applied to the optimization of the geometries and vibration frequencies of all species. A detailed study of the likely routes associated with PCDD/F formation via aliphatic hydrocarbons as precursors is presented. To provide data support for the establishment of a mathematical model of environmental monitoring, Arrhenius formulas were fit in the temperature range 300–1300 K. The results presented here could be used to evaluate the contribution of aliphatic hydrocarbons acting as a precursor to PCDD/Fs formation.

Computational methods

The DFT [16, 17] was used to calculate the spatial structural parameters of reactants, transition states (TS), intermediates and products involved in the elementary reaction path at the B3LYP level of theory [18] with 6-311 + G (d, p) taken as the basis set. The stability and reliability of the calculation method and basis group have been verified by Dar et al. [19]. To locate the TS, we used the TS algorithm based on the initial guess. An intrinsic reaction coordinate (IRC) calculation was carried out to ensure that the TS structure and the corresponding reactants and products or intermediates were associated. To confirm the stability of the structure, frequency analysis was carried out for all the stationary structures involved, ensuring that the reactants, intermediates and products do not appear with virtual frequency. The TS has only one imaginary frequency, which guarantees the uniqueness of the TS structure. Free energies and thermochemical enthalpies were calculated at B3LYP/6-311 + G(d, p) level of theory, and the correction of the zero point energy (ZPE) was taken into account. The variational transition state theory (VTST) was clearly advantageous in the case of higher temperature and lower potential barrier [20]. The VTST was used to calculate the rate constants of chemical reactions for the critical elementary reactions and tunnel effects were taken into account to correct the calculation results. All of the quantum chemical calculations were carried out with Gaussian09 program suite on the model of ServMaxPSC-201GAMAX server.

Results and discussion

Formation of 2-CPR and 3-CPR by aliphatic hydrocarbons

Formation of 2-CP and 3-CP by aliphatic hydrocarbons

The gas-phase reaction mechanisms of benzene formation via ethylene, acetylene, propylene and butylene(1-butene and 2-butene) are depicted in Fig. 1. The calculation results demonstrate that three C_2H_4 can generate the intermediate cyclohexane via cyclic polymerization. In ethylenes, double bond rupture and ring closure occur in a one-step reaction through transition state TS1 then forming IM1, subsequently generating IM2 cyclohexene via intra-annular elimination of H_2. Via the intra-annular elimination of H_2, IM2 could be through two paths: IM2 eliminates para-position H_2 to generate IM3 or ortho-position H_2 to generate IM4, both of which are endothermic reactions, have a relatively larger potential barrier. The potential barrier of elimination of H_2 from IM4 is significantly higher than that from IM3, mainly because the steric hindrance effect of the ortho C–H bond is higher than that of the para position. Furthermore, benzene can be formed via three acetylene cyclization. The potential barrier is 59.24 kcal mol^{-1}, which is a strong exothermic process.

Intra-annular elimination of H_2 from two propylenes forms IM7, which requires a high potential barrier of 98.52 kcal mol^{-1} and is strongly endoergic by 98.52 kcal mol^{-1}. The elimination of H from IM7 appears to be barrierless, and more strongly endoergic than the last step. Two IM8 molecules then undergo ring closure to generate benzene, and the reaction heat released by this process is far less than that of acetylene cyclization to benzene. We analyzed aromatizing 1-butene and 2-butene to benzene simultaneously; 1,3-butadiene could be produced via the stepwise elimination α-H and β-H of 1-butene or the elimination of intra-annular H_2 in 2-butene. The calculated results illustrate that the potential barrier of elimination α-H is much lower than that of β-H, but the reaction heats are just the opposite. In addition, the potential barrier of simultaneous removal α-H and β-H is much higher than that of stepwise elimination of H. 2-Butene could generate IM6 directly via eliminating two indentical α-H; the potential barrier is significantly lower than that of 1-butene direct elimination of α-H and β-H to generate IM6, and the reaction heats do not differ much, which indicates that the reaction from 2-butene to IM6 occurs more easily. IM6 and acetylene can be cyclized to produce cyclohexadienyl, which is a strongly endothermic reaction,

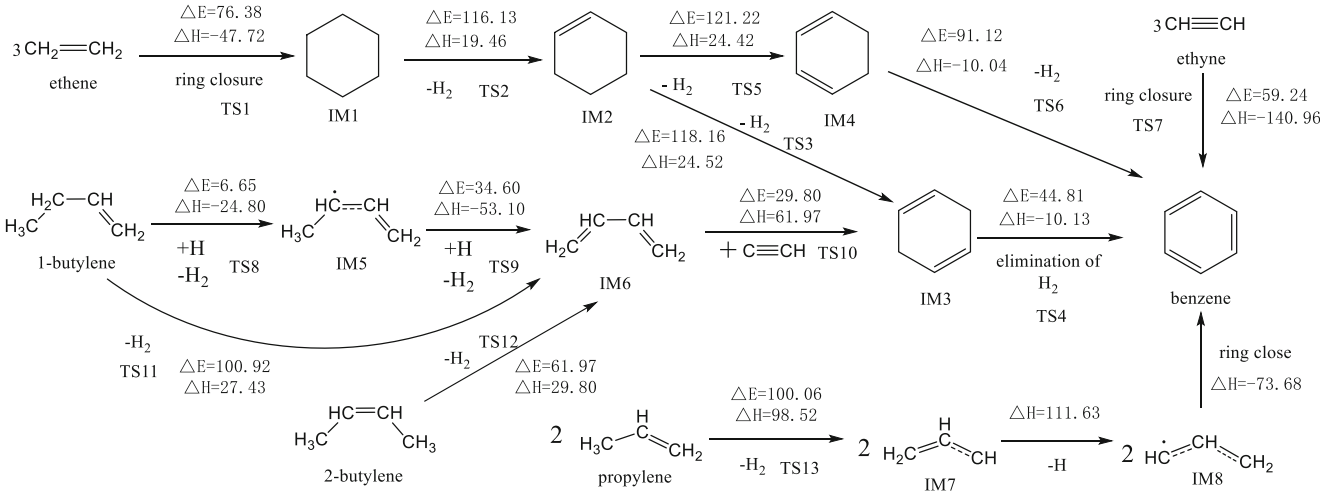

Fig. 1 Formation routes of benzene through the small molecule aliphatic hydrocarbons (ΔE potential barriers, kcal mol^{-1}; ΔH reaction heats, kcal mol^{-1}; 298.15 K)

then IM3, through removing the para position two H and intra-annular rearrangement reaction generates benzene.

In the process of preparation of industrial phenol, benzene can be directly oxidized to phenol by oxidizing agents such as O_2 and H_2O_2 [21, 22]. The main mechanism is as follows: the hydroxyl radical formed by H_2O_2 will attack the benzene ring, forming the intermediate hydroxyl radical and then phenol [23].

The reaction route of benzene to chlorophenol may also have a similar reaction path in the complex waste incineration process. The formation scheme embedded with potential barriers and reaction heats is shown in Fig. 2, and the TS structures are shown in supporting information Fig. S5. The chlorobenzene formation with Cl_2 as chlorine source provides Cl to substitute H in benzene, which meanwhile needs to cross a higher barrier. Chlorobenzene may be oxidized directly by oxygen under complicated conditions to produce IM9, which is further reduced by H_2, undergoing intramolecular H migration to then produce 2-chlorophenol (2-CP) or 3-chlorophenol (3-CP) via intramolecular dehydration. H-shift dehydration is the rate-determining step. The other route is OH radical attacking chlorobenzene to form IM11 and IM12, which occurs easily due as the potential barrier of this elementary reaction is relatively small, only about 8 kcal mol^{-1}. The H atom in IM11 is abstracted by H, Cl or OH to form 2-chlorophenols (2-CP) or 3-chlorophenols (3-CP). The elementary reaction is a strongly exothermic reaction, where the potential barrier of the H free radical extraction is 22–26 kcal mol^{-1}, Cl or OH free radical extraction reactions appear to be barrierless. In comparison, the potential barrier of pathway 3 and 4 is much higher than that of pathway 1 and 2; besides, the potential barrier of elimination H in IM11 via H is significantly higher than Cl and OH, which are both barrierless in pathway 1 and 2 and pathway 3 and 4 are homologous and competitive.

Formation of 2-CPR and 3-CPR by chlorophenol

Previous studies have shown that PCDD/Fs can be formed by radicals–radicals, radicals–molecules, and chlorophenols molecules [24]. Among them, the reaction between phenoxy radicals is dominant. Chlorinated phenoxy radicals are classified as persistent organic pollutants because they are difficult to decompose and have strong toxicity. At the same time, their reactivity with other substances, especially reactive oxygen, is relatively low, so they can be used as precursors to generate PCDD/Fs [25]. Formation of the phenoxy radical is one of the most important steps for homogeneous reaction to produce PCDD/Fs [24]. Therefore, we studied the formation mechanism of PCDD/Fs via phenoxy radical and primarily calculated the potential barriers and reaction heats of phenoxy radicals formation via 2-CP and 3-CP. In particular, the total energy of the TS energy obtained by Cl extraction via ZPE correction is lower than the total energy for the reactant chlorophenol with Cl, so the reaction is barrierless. The calculation results are consistent with those obtained by Zhang Qingzhu et al. [26] at the MPWB1K/6-311 + G (3df, 2p) level to extract Cl on 2,4-DCPR and 2,4,6-TCP. The reaction potential barrier and reaction heats (both include ZPE correction) are shown in Table 1.

Formation of PCDD/Fs from 2-CPR and 3-CPR

Formation of PCDDs from 2-CPR and 3-CPR

This section gives six possible paths for the formation of PCDDs, which are formed by 2-CPR and 3-CPR. The formation schemes embedded with the potential barriers and reaction heats are depicted in Fig. 3. The TS structures involved in the reaction are shown in supporting information Fig. S6. The basic process of the formation of PCDDs by phenoxy radicals includes the following elementary processes: carbon–oxygen

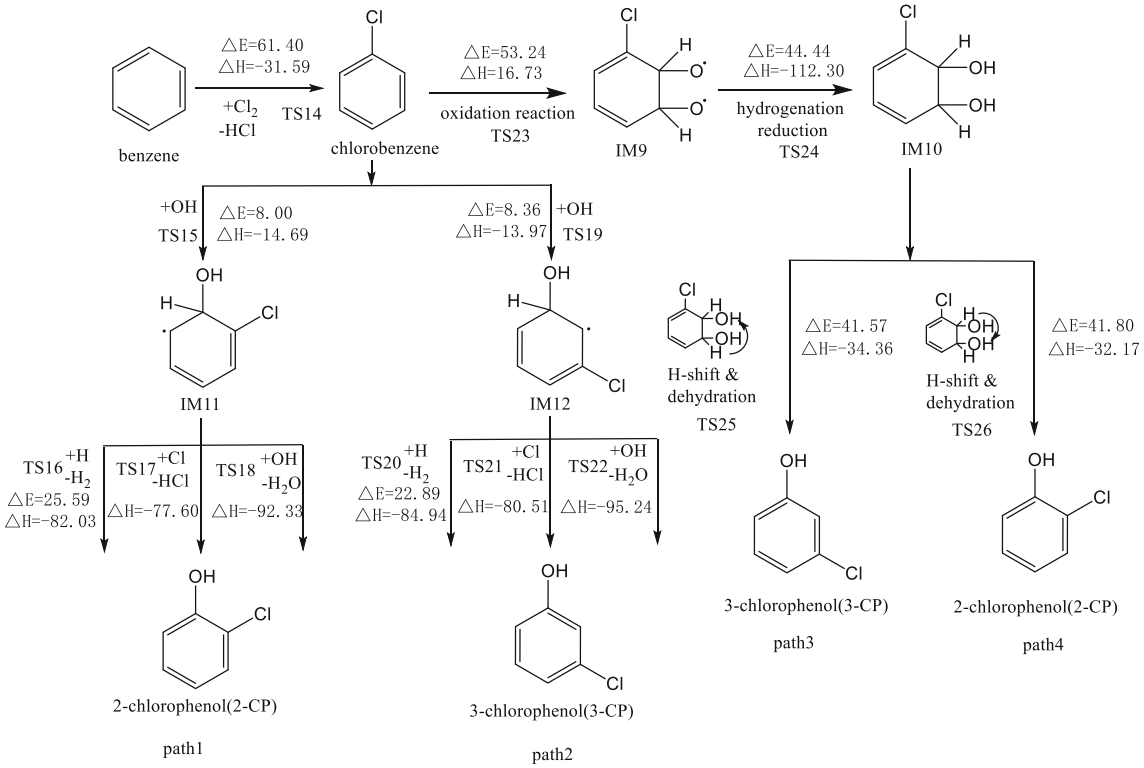

Fig. 2 Formation routes of 2-phenol and 3-phenol from benzene (ΔE potential barriers, kcal mol^{-1}; ΔH reaction heats, kcal mol^{-1}, 298.15 K)

coupling dimerization, H abstraction, ring closure and the intra-annular elimination of H. In the elementary process of 1,6-DCDD formation, the carbon–oxygen coupling dimerization between two 2-CPRs is barrierless and exothermic by 14.95 kcal mol^{-1}. The potential barrier of process about abstracting H from IM1 by high-energy H radical is greater than the OH radical, but with less reaction heat.

The dimerization process of two 3-CPR via carbon–oxygen coupling occurs in three ways. However, due to the different positions of aromatic ring Cl substitution, the electronic and steric hindrance effects differ during the formation of PCDDs. The potential barrier of H abstraction in the formation of 1,6-DCDD is higher than that in 1,8-DCDD, 2,7-DCDD; however, the abstraction characteristics of OH radical are opposite to this. The main reason is that the Cl substitution site is closer to the H atom to be eliminated, and the decrease in electron density on the benzene ring promotes nucleophilic attack of O in the OH free radical. The reaction heats of IM4 to IM5 are lower than that from IM7 to IM8 and from IM10 to IM11, and the gap in elementary reaction heats is very small in the latter two steps. The ring closure process is an endothermic reaction, and the potential barrier and reaction heat of 1,6-DCDD and 1,8-DCDD are similar but greater than those of 2,7-DCDD. The most likely reason is that the presence of vicinal Cl atoms increase the barrier of ring closure. H elimination is the rate-determining step in the chain with highest potential barrier and strongly endothermic. The calculated results show that the reaction heat and reaction potential barrier approximation in the formation of 1,6-DCDD and 1,8-DCDD, respectively 31.20 kcal mol^{-1}, 31.23 kcal mol^{-1} and 27.53 kcal mol^{-1}, 27.55 kcal mol^{-1} and greater than that of 2,7-DCDD. Therefore, it can be inferred that the substitution position of Cl has a great influence on the barrier and reaction heat of the elementary reaction.

The formation of 1,9-DCDD and 3,9-DCDD may have two reaction paths by 2-CPR and 3-CPR cross coupling. The difference between the carbon–oxygen coupling dimerization sites determines the difference in the product and the reaction mechanism is similar to that of the previous chlorophenoxy free radicals. Comparing path 1 to path 4, it was found that the reaction heat of the 2-CPR and 3-CPR cross-carbon-oxygen

Table 1 The potential barriers (ΔE) and reaction heats (ΔH) for the formation of the 2-CPR and 3-CPR from 2-CP and 3-CP through various processes

Reactions	ΔE (kcal mol^{-1})	ΔH (kcal mol^{-1})
2-CP → 2CPR + H	Barrierless	81.59
2-CP + H → 2CPR + H_2	7.92	−22.96
2-CP + Cl → 2CPR + HCl	Barrierless	−18.54
2-CP + OH → 2CPR + H_2O	2.02	−33.26
3-CP → 3CPR + H	Barrierless	83.84
3-CP + H → 3CPR + H_2	9.32	−20.70
3-CP + Cl → 3CPR + HCl	Barrierless	−16.28
3-CP + OH → 3CPR + H_2O	1.81	−31.00

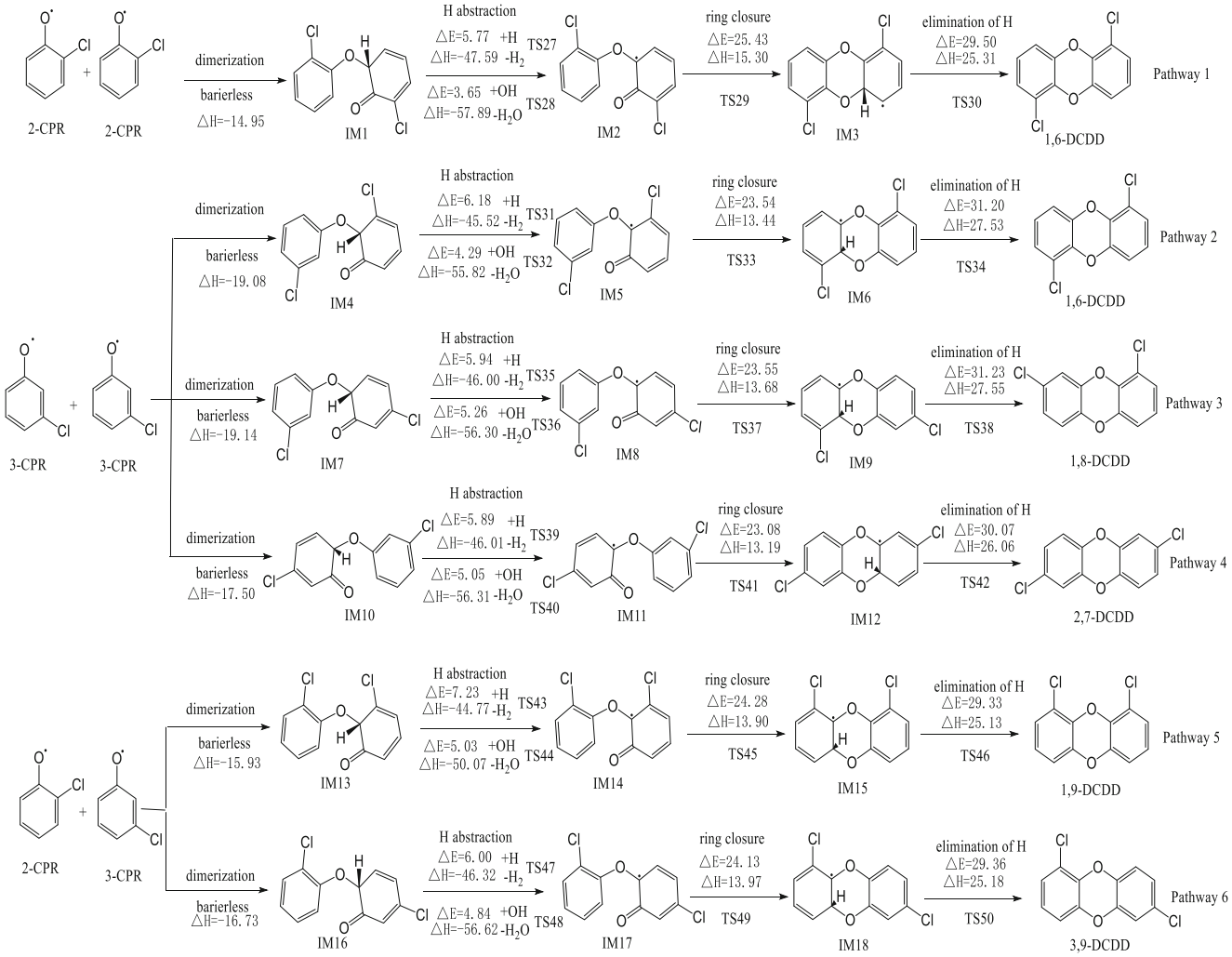

Fig. 3 Formation routes of polychlorinated dibenzodioxins (PCDDs) embedded with the potential barriers ΔE (kcal mol^{-1}) and reaction heats ΔH (kcal mol^{-1}) from 2-CPR and 3-CPR precursors

coupling dimerization was between the reaction of two 2-CPRs and two 3-CPRs. The substitution position of Cl in the aromatic ring has a certain effect on the abstraction of H from aromatic hydrocarbons, which also improves the extraction barrier of the H radical and reduces the extraction barrier of the OH radical. The calculated results show that the reaction heat of the elementary reaction abstracted H from the carbon–oxygen coupling dimer is the maximum in the reaction path and the potential barrier of the final H-elimination reaction is the largest, making this the rate-determining step of the routes. Taken all together, the six pathways are analogous and competitive.

Formation of PCDFs from 2-CPR and 3-CPR

Studies by Werber et al. [4] showed that the formation of the intermediate dioxo-dichloro-biphenyl by the coupling of the vicinal C–C atom of the phenoxy radical is a key elementary reaction for the formation of polychlorinated biphenyls and furans. The main elementary reactions that form PCDFs based on 2-CPR and 3-CPR include: the coupling reactions of different phenoxy radicals between vicinal carbon atoms, the abstraction of H or Cl, the migration rearrangement of single H atom, ring closure, and OH elimination. There are four reaction paths for the formation of PCDFs with 2-CPR and 3-CPR as precursors. The formation schemes embedded with the potential barriers and reaction heats are shown in Fig. 4, and the TS structures are shown in supporting information Fig. S7.

The first step in the fomation of PCDFs is carbon–carbon coupling dimerization, which appears to be barrierless and significantly less exothermic compared to the carbon–oxygen coupling dimerization involved in PCDD formation. From the comparison, we find that the reaction heat of carbon–carbon coupling dimerization occurring on the C attached to the Cl atom substituent is lower than when not attached to the Cl atom. Using H and OH radicals to extract Cl of the dimer coupling sites, the calculated results show that the reaction

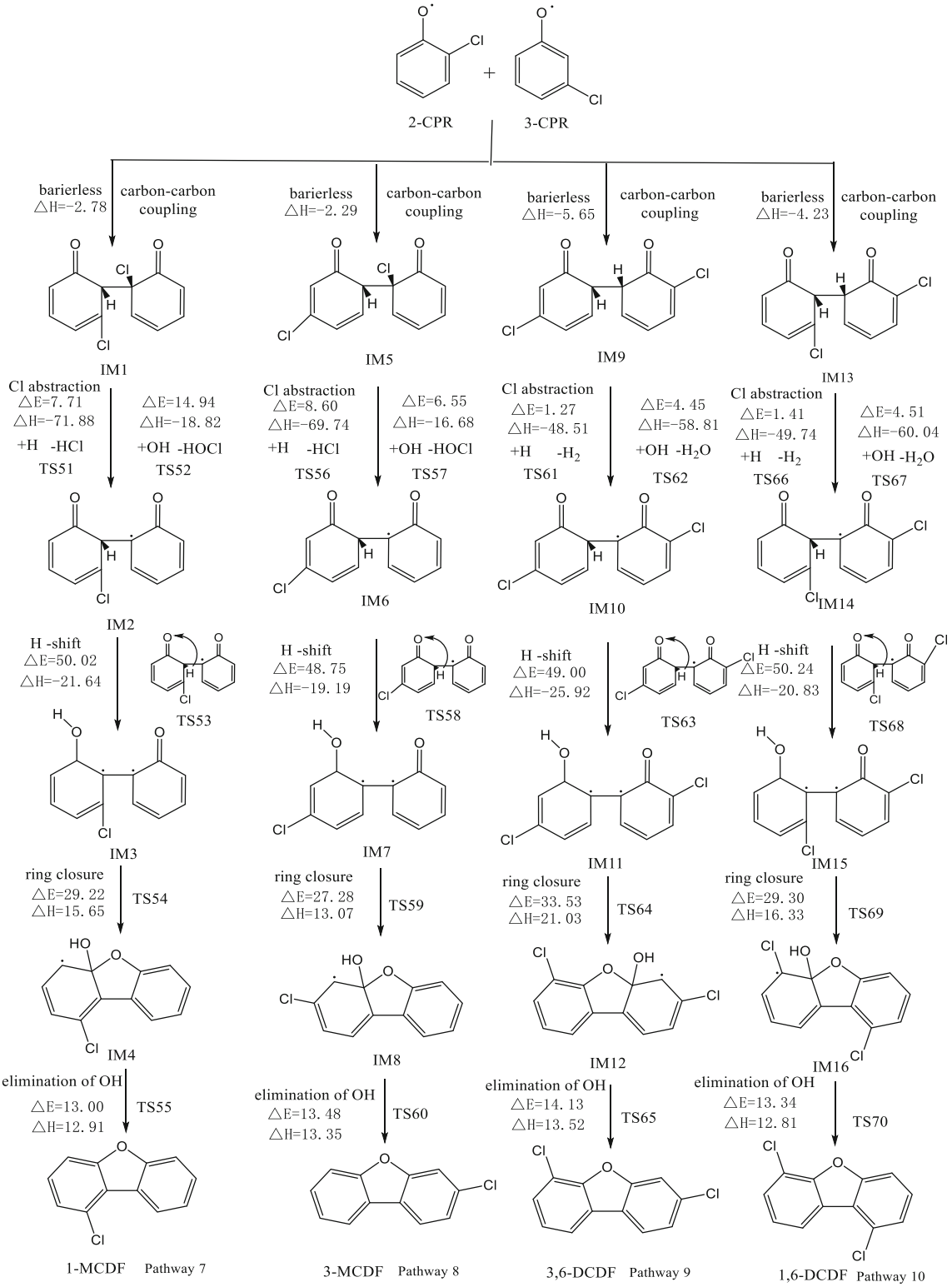

Fig. 4 Formation routes of polychlorinated dibenzofurans (PCDFs) embedded with the potential barriers ΔE (kcal mol^{-1}) and reaction heats ΔH (kcal mol^{-1}, 298.15 K) from 2-CPR and 3-CPR precursors

heat and reactivity barrier of the elemental reaction have a very good relationship with the molecular structure. Cl abstraction is exothermic, the reaction heat by high energy H extraction to produce HCl is higher than that by OH radical extraction to produce HOCl, and the potential barrier of OH extraction is higher than that of H. Reduced stability of H in

the carbon–carbon coupling site and the H atom migrates from the carbon–carbon coupling site to the O atom on aromatic hydrocarbons, then generates a phenolic hydroxyl group, which is an exothermic reaction and the rate-determining step in PCDF formation. The potential barrier of the ring closure step in the formation of PCDFs is slightly higher compared with that in the formation of PCDDs. The potential barrier of the rate-determining step in the formation of PCDFs is larger, indicating that the amount of PCDFs generated by the precursor is less than PCDDs under the same conditions.

Rate constant calculations

A mathematical model was established to study the potential results of pollutants released into environment and to provide relevant guidance for environmental monitoring and risk decision analysis. Pre-exponential factor, activation energy and rate constant in the Arrhenius equation were obtained during the formation of PCDD/Fs, which matters in establishment of the mathematical model. The rate constants of the elementary reactions involved in the formation of PCDD/Fs from small molecule aliphatic hydrocarbon precursors were evaluated by the VTST over a wide temperature range from 300 to 1300 K. Meanwhile, the rate constants of relevant elementary reactions were fitted. Since there is very little in the literature so far showing the direct correlation between experimental values and theoretical values, in order to verify the accuracy of the fitting formula, we compare with the previous calculated results by Gao et al. Zhang et al. [26, 27] at MPWB1K/6-311 + G (3DF, 2P) level on similar reactions, as well as the analysis of chemical reaction rate constants obtained in CVT/SCT fitting. It turns out that the magnitudes of parameters between similar reactions are the same. For instance, the pre-exponential factor of 2-CP + H → 2-CPR + H_2 was 3.13×10^{-11} s^{-1}, while the pre-exponential factor of 2,4-DCP + H → 2,4-DCPR+H_2 by Zhang was 5.01×10^{-11} s^{-1}. The pre-exponential factor of the 1,6-DCDD loop closing reaction IM6 → 1,6-DCDD+H is $4.92 \times 10^{13} s^{-1}$, Zhang et al. [27]

Table 2 Arrhenius formulas for elementary reactions involved in formation of 2-CPR and 3-CPR from small molecule aliphatic hydrocarbon over the temperature range 300–1300 K[a]

Reaction	Arrhenius formula
$3C_2H_2 \rightarrow C_6H_6$	$k(T) = (1.97 \times 10^{59})\exp.(-31{,}092.19/T)$
$3C_2H_4 \rightarrow$ IM1	$k(T) = (5.63 \times 10^{47})\exp.(-39{,}662.87/T)$
IM1 → IM2 + H_2	$k(T) = (1.36 \times 10^{14})\exp.(-59{,}228.89/T)$
IM2 → IM3 + H_2	$k(T) = (3.34 \times 10^{14})\exp.(-61{,}920.67/T)$
IM2 → IM4 + H_2	$k(T) = (2.11 \times 10^{15})\exp.(-60{,}801.91/T)$
IM3 → C_6H_6 + H_2	$k(T) = (7.72 \times 10^{13})\exp.(-45{,}951.17/T)$
IM4 → C_6H_6 + H_2	$k(T) = (5.94 \times 10^{12})\exp.(-22{,}333.65/T)$
C_4H_8 + H → IM5 + H_2	$k(T) = (6.35 \times 10^{-11})\exp.(-3679.19/T)$
IM5 + H → IM6 + H_2	$k(T) = (5.87 \times 10^{-13})\exp.(-17{,}266.57/T)$
IM6 + C_2H_2 → IM3	$k(T) = (1.59 \times 10^{-12})\exp.(-16{,}648.70/T)$
1-C_4H_8 → IM6 + H_2	$k(T) = (6.74 \times 10^{+13})\exp.(-53{,}961.05/T)$
2-C_4H_8 → IM6 + H_2	$k(T) = (9.88 \times 10^{+11})\exp.(-30{,}937.75/T)$
C_3H_6 → IM7 + H_2	$k(T) = (4.59 \times 10^{+14})\exp.(-51{,}460.42/T)$
C_6H_6 + Cl_2 → C_6H_5Cl + HCl	$k(T) = (2.01 \times 10^{-06})\exp.(-34{,}356.93/T)$
C_6H_5Cl + O_2 → IM9	$k(T) = (4.56 \times 10^{-14})\exp.(-27{,}451.47/T)$
IM9 + H_2 → IM10	$k(T) = (5.82 \times 10^{-12})\exp.(-22{,}357.86/T)$
IM10 → 2-CP + H_2O	$k(T) = (6.94 \times 10^{13})\exp.(-21{,}526.85/T)$
IM10 → 3-CP + H_2O	$k(T) = (5.28 \times 10^{13})\exp.(-21{,}342.42/T)$
C_6H_5Cl + OH → IM11	$k(T) = (1.84 \times 10^{-12})\exp.(-4771.84/T)$
IM11 → 2-CP + H_2	$k(T) = (1.36 \times 10^{-12})\exp.(-12{,}355.25/T)$
C_6H_5Cl + OH → IM12	$k(T) = (1.98 \times 10^{-12})\exp.(-4954.97/T)$
IM12 → 3-CP + H_2	$k(T) = (1.70 \times 10^{-12})\exp.(-11{,}002.35/T)$
2-CP + H → 2-CPR + H_2	$k(T) = (3.13 \times 10^{-11})\exp.(-4192.60/T)$
2-CP + OH → 2-CPR + H_2O	$k(T) = (1.33 \times 10^{-12})\exp.(-1908.51/T)$
3-CP + H → 3-CPR + H_2	$k(T) = (5.74 \times 10^{-11})\exp.(-4712.50/T)$

[a] Units are s^{-1} and cm^3 mol^{-1} s^{-1} for unimolecular and bimolecular reactions

Table 3 Arrhenius formulas for elementary reactions involved in formation of PCDDs from 2-CPR and 3-CPR over the temperature range of 300-1300 K[a]

Reaction	Arrhenius formula
IM1 + H → IM2 + H_2	$k(T) = (1.13 \times 10^{-10})\exp.(-3370.33/T)$
IM1 + OH → IM2 + H_2O	$k(T) = (2.42 \times 10^{-12})\exp.(-2691.81/T)$
IM2 → IM3	$k(T) = (4.36 \times 10^{11})\exp.(-12{,}769.06/T)$
IM3 → 1,6-DCDD+H	$k(T) = (4.33 \times 10^{13})\exp.(-15{,}335.73/T)$
IM4 + H → IM5 + H_2	$k(T) = (2.46 \times 10^{-11})\exp.(-3508.14/T)$
IM4 + OH → IM5 + H_2O	$k(T) = (2.43 \times 10^{-12})\exp.(-3041.37/T)$
IM5 → IM6	$k(T) = (3.94 \times 10^{11})\exp.(-11{,}786.02/T)$
IM6 → 1,6-DCDD+H	$k(T) = (4.92 \times 10^{13})\exp.(-16{,}232.63/T)$
IM7 + H → IM8 + H_2	$k(T) = (9.71 \times 10^{-11})\exp.(-3456.84/T)$
IM7 + OH → IM8 + H_2O	$k(T) = (6.52 \times 10^{-12})\exp.(-3553.44/T)$
IM8 → IM9	$k(T) = (4.33 \times 10^{11})\exp.(-11{,}806.09/T)$
IM9 → 1,8-DCDD+H	$k(T) = (5.04 \times 10^{13})\exp.(-16{,}252.82/T)$
IM10 + H → IM11 + H_2	$k(T) = (1.08 \times 10^{-10})\exp.(-3429.39/T)$
IM10 + OH → IM11 + H_2O	$k(T) = (9.46 \times 10^{-12})\exp.(-3470.08/T)$
IM11 → IM12	$k(T) = (3.44 \times 10^{11})\exp.(-11{,}545.44/T)$
IM12 → 2,7-DCDD+H	$k(T) = (4.21 \times 10^{13})\exp.(-15{,}641.53/T)$
IM13 + H → IM14 + H_2	$k(T) = (2.18 \times 10^{-11})\exp.(-4025.22/T)$
IM13 + OH → IM14 + H_2O	$k(T) = (7.89 \times 10^{-13})\exp.(-3369.27/T)$
IM14 → IM15	$k(T) = (3.46 \times 10^{11})\exp.(-12{,}157.83/T)$
IM15 → 1,9-DCDD+H	$k(T) = (4.43 \times 10^{13})\exp.(-15{,}250.66/T)$
IM16 + H → IM17 + H_2	$k(T) = (8.70 \times 10^{-11})\exp.(-3476.07/T)$
IM16 + OH → IM7 + H_2O	$k(T) = (4.62 \times 10^{-12})\exp.(-3309.17/T)$
IM17 → IM18	$k(T) = (3.81 \times 10^{11})\exp.(-12{,}091.77/T)$
IM18 → 3,9-DCDD+H	$k(T) = (4.54 \times 10^{13})\exp.(-15{,}266.94/T)$

[a] Units are s^{-1} and cm^3 mol^{-1} s^{-1} for unimolecular and bimolecular reactions

Table 4 Arrhenius formulas respectively for elementary reactions involved in formation of PCDFs from 2-CPR and 3-CPR over the temperature range 300–1300 K

Reaction	Arrhenius formula
IM1 + H → IM2 + HCl	$k(T) = (2.53 \times 10^{-10})\exp.(-4464.89\ /T)$
IM1 + OH → IM2 + HClO	$k(T) = (4.13 \times 10^{-12})\exp.(-8360.33\ /T)$
IM2 → IM3	$k(T) = (3.86 \times 10^{12})\exp.(-24{,}977.08\ /T)$
IM3 → IM4	$k(T) = (5.50 \times 10^{12})\exp.(-14{,}922.36\ /T)$
IM4 → 1-MCDF+OH	$k(T) = (5.52 \times 10^{13})\exp.(-7008.57\ /T)$
IM5 + H → IM6 + HCl	$k(T) = (5.15 \times 10^{-10})\exp.(-4904.63\ /T)$
IM5 + OH → IM6 + HClO	$k(T) = (7.27 \times 10^{-12})\exp.(-4182.56\ /T)$
IM6 → IM7	$k(T) = (3.26 \times 10^{12})\exp.(-24{,}351.49\ /T)$
IM7 → IM8	$k(T) = (1.05 \times 10^{12})\exp.(-13{,}695.47\ /T)$
IM8 → 3-MCDF+OH	$k(T) = (5.59 \times 10^{13})\exp.(-7258.96\ /T)$
IM9 + H → IM10 + H_2	$k(T) = (6.48 \times 10^{-11})\exp.(-1107.20\ /T)$
IM9 + OH → IM10 + H_2O	$k(T) = (1.71 \times 10^{-12})\exp.(-2948.87\ /T)$
IM10 → IM11	$k(T) = (3.78 \times 10^{12})\exp.(-24{,}489.42\ /T)$
IM11 → IM12	$k(T) = (8.38 \times 10^{12})\exp.(-17{,}218.62\ /T)$
IM12 → 3,6-MCDF+OH	$k(T) = (5.28 \times 10^{13})\exp.(-7573.52\ /T)$
IM13 + H → IM14 + H_2	$k(T) = (1.68 \times 10^{-14})\exp.(-423.99\ /T)$
IM13 + OH → IM14 + H_2O	$k(T) = (1.17 \times 10^{-11})\exp.(-3257.62\ /T)$
IM14 → IM15	$k(T) = (4.84 \times 10^{12})\exp.(-25{,}103.52\ /T)$
IM15 → IM16	$k(T) = (4.49 \times 10^{12})\exp.(-14{,}943.99\ /T)$
IM16 → 1,6-MCDF+OH	$k(T) = (5.42 \times 10^{13})\exp.(-7175.13\ /T)$

Units are s^{-1} and $cm^3\ mol^{-1}\ s^{-1}$ for unimolecular and bimolecular reactions

fitted the Arrhenius formulas obtained from the formation of 1,3,8-TCDD and 1,3,6,8-TCDD by double 2,3-DCPR molecules. The pre-exponential factors of the loop closing reaction were $8.94 \times 10^{12} s^{-1}$ and $3.17 \times 10^{13} s^{-1}$, respectively. Therefore, the rate constants we calculated are reliable.

The rate constants of the elementary reactions involved in the formation of PCDD/Fs from the small molecule aliphatic hydrocarbon precursors were evaluated over a wide temperature range from 300 to 1300 K and the Arrhenius equations are shown in Tables 2, 3 and 4. Pre-exponential factor, activation energy and rate constants can be obtained from these Arrhenius formulas.

Conclusions

Based on the DFT theory, we have studied the gas-phase reaction mechanism of PCDD/Fs formation in two stages with aliphatic hydrocarbons as precursors. In the first stage, all elementary reactions have a very high potential barrier. Reaction heats of carbon–oxygen coupling dimerization between phenoxy radicals is much larger than that of carbon–carbon coupling dimerization. The substitution position of Cl has a certain effect on the potential barrier and reaction heats. The elementary reaction of intramolecular H removal is the determining step in the second stage reaction of PCDDs and PCDFs formation. In general, aliphatic hydrocarbons such as C_2H_2, C_2H_4, C_3H_6, C_4H_8 have low reactivity when serving as dioxin precursors. Therefore, in practical applications, pretreatment of sewage sludge could be carried out to minimize the content of chlorinated compounds and metals. The original sludge can then be made into a waste-derived RDF (refuse-derived fuel), which can be used for subsequent incineration [28].

Acknowledgments This work was supported by Beijing Natural Science Foundation (2182066), Natural Science Foundation of Hebei Province of China (B2018502067).

References

1. Folgueras MB, Alonso M, Díaz RM (2013) Influence of sewage sludge treatment on pyrolysis and combustion of dry sludge. Energy 55:426–435
2. Harrison EZ, Oakes SR, Hysell M, Hay A (2006) Organic chemicals in sewage sludges. Sci Total Environ 367:481
3. Singh A, Agrawal M (2008) Acid rain and its ecological consequences. J Environ Biol 29:15–24
4. Weber R, Hagenmaier H (1999) Mechanism of the formation of polychlorinated dibenzo-p-dioxins and dibenzofurans from chlorophenols in gas phase reactions. Chemosphere 38:529–549
5. Choate CE (2010) Systems and methods for combining and converting solid and liquid organic waste materials into useful products
6. Margallo M, Taddei MBM, Hernández-Pellón A, Aldaco R, Irabien Á (2015) Environmental sustainability assessment of the management of municipal solid waste incineration residues: a review of the current situation. Clean Techn Environ Policy 17:1333–1353
7. Shibamoto T, Yasuhara A, Katami T (2007) Dioxin formation from waste incineration. Rev Environ Contam Toxicol 190:1–41
8. Park MH, Kim HJ, Lee MG, Park SH, Lee YC, Chung DY (2011) Nature and fate of dioxin in soil environment. Korean J Soil Sci Fert 44:657–661
9. Lambert MK, Friedman C, Luey P, Lohmann R (2011) Role of black carbon in the sorption of polychlorinated dibenzo-p-dioxins and dibenzofurans at the diamond alkali superfund site, Newark Bay, New Jersey. Environ Sci Technol 45:4331–4338
10. Sun Y, Sun Y, Wang D (2016) Research on revision of dioxin exhaust emission factor from waste incineration industry. Environ Sci Manag
11. Zhao X, Zhu W, Huang J, Li M, Gong M (2015) Emission characteristics of PCDD/fs, PAHs and PCBs during the combustion of sludge-coal water slurry. J Energy Inst 88:105–111
12. Addink R, Bakker WCM, Olie K (1995) Influence of HCl and Cl2 on the formation of polychlorinated dibenzo-p-dioxins/dibenzofurans in a carbon/fly ash mixture. Environ Sci Technol 29:2055–2058
13. Ke S, Yan JH, Li XD, Lu SY, Wei YL, Fu MX (2010) Experimental study on the effects of H(2)O on PCDD/Fs formation by de novo synthesis in carbon/CuCl(2) model system. Chemosphere 78:672
14. Qu X, Wang H, Zhang Q, Shi X, Xu F, Wang W (2009) Mechanistic and kinetic studies on the homogeneous gas-phase formation of PCDD/fs from 2,4,5-trichlorophenol. Environ Sci Technol 43:4068–4075

15. Khachatryan L, Ruben Asatryan A, Dellinger B (2011) An elementary reaction kinetic model of the gas-phase formation of polychlorinated dibenzofurans from chlorinated phenols. J Phys Chem A 108:9567–9572
16. Yang X, Liu H, Hou H, Flamm A, Zhang X, Wang Z (2010) Studies of thermodynamic properties and relative stability of a series of polyfluorinated dibenzo-p-dioxins by density functional theory. J Hazard Mater 181:969
17. Qu R, Liu H, Zhang Q, Flamm A, Yang X, Wang Z (2012) The effect of hydroxyl groups on the stability and thermodynamic properties of polyhydroxylated xanthones as calculated by density functional theory. Thermochim Acta 527:99–111
18. Lee C, Yang W, Parr RG (1988) Development of the Colle-Salvetti correlation-energy formula into a functional of the electron density. Phys Rev B Condens Matter 37:785–789
19. Dar T, Shah K, Moghtaderi B, Page AJ (2016) Formation of persistent organic pollutants from 2,4,5-trichlorothiophenol combustion: a density functional theory investigation. J Mol Model 22: 1471–1475
20. Truhlar DG, Garrett BC, Hipes PG, Kuppermann A (1984) Test of variational transition state theory against accurate quantal results for a reaction with very large reaction-path curvature and a low barrier. J Chem Phys 81:3542–3545
21. Yamanaka H, Hamada R, Nibuta H, Nishiyama S, Tsuruya S (2002) Gas-phase catalytic oxidation of benzene over cu-supported ZSM-5 catalysts: an attempt of one-step production of phenol. J Mol Catal A Chem 178:89–95
22. Kato CN, Hasegawa M, Sato T, Yoshizawa A, Inoue T, Mori W (2005) Microporous dinuclear copper (II) trans-1, 4-cyclohexanedicarboxylate: heterogeneous oxidation catalysis with hydrogen peroxide and X-ray powder structure of peroxo copper (II) intermediate. J Catal 230:226–236
23. Vilhunen S, Puton J, Virkutyte J, Sillanpää M (2011) Efficiency of hydroxyl radical formation and phenol decomposition using UV light emitting diodes and H2O2. Environ Technol 32:865–872
24. Dar T, Altarawneh M, Dlugogorski BZ (2012) Theoretical study in the dimerisation of 2-chlrothiophenol/2-chlorothiophenoxy: precursors to PCDT/TA. Organohalogen Compd 74:657–660
25. Altarawneh M, Dlugogorski BZ, Kennedy EM, Mackie JC (2009) Mechanisms for formation, chlorination, dechlorination and destruction of polychlorinated dibenzo-p-dioxins and dibenzofurans (PCDD/fs). Prog Energ Combust 35:245–274
26. Zhang Q, Yu W, Zhang R, Zhou Q, Gao R, Wang W (2010) Quantum chemical and kinetic study on dioxin formation from the 2,4,6-TCP and 2,4-DCP precursors. Environ Sci Technol 44: 3395–3403
27. Gao R, Xu F, Li S, Hu J, Zhang Q, Wang W (2013) Formation of bromophenoxy radicals from complete series reactions of bromophenols with H and OH radicals. Chemosphere 92:382–390
28. Kupka T, Mancini M, Irmer M, Weber R (2008) Investigation of ash deposit formation during co-firing of coal with sewage sludge, sawdust and refuse derived fuel. Fuel 87:2824–2837